Visualization of three-dimensional flow structures around a wall-mounted short cylinder

Hiroka RINOSHIKA[1], Akira RINOSHIKA[1,2,*] and Jin-Jun WANG[2]

[1] Department of Mechanical Systems Engineering, Yamagata University, Yamagata, JAPAN
[2] School of Aeronautic Science and Engineering, Beijing University of Aeronautics and Astronautics, Beijing, China
*corresponding author: rinosika@yz.yamagata-u.ac.jp

Abstract Three-dimensional (3D) flow structures around a wall-mounted short cylinder of an aspect ratio 1 were instantaneously measured by a high-resolution Tomographic particle image velocimetry (TPIV) in a water tunnel. Here both of the diameter D and height H of the cylinder is 70 mm. Tomographic PIV measurement was performed at Reynolds number of 8,570 according to the diameter of the cylinder by using four high-resolution double-exposure CCD cameras. Based on the measured instantaneous 3D velocity distribution, 3D velocity fields, the vorticity, the Q criterion, the rear separation region and the characteristic of arch type vortex and tip vortices are firstly discussed. This paper found a 3D W-type arch vortex behind the short cylinder, which is originated by the interaction between upwash and downwash flows. The head shape of arch vortex structure does not only depend on the aspect ratio of the cylinder, but also is associated with the cylinder diameter.
Keywords: Arch vortex, Three-dimensional flow structure, Tomographic PIV, Vortex, finite cylinder

1 Introduction

A strongly three-dimensional (3D) complex flow structure is originated by a finite circular cylinder, and the aspect ratio of the cylinder, i.e., the ratio of the height and diameter, has significant effect on the wake structure. It is different from the structure of an infinite circular cylinder [1], [2], owning to the effect of the cylinder free end and the connection between cylinder and ground plane [3]-[6]. The engineering field has many important applications, such as reducing drag and noise induced by designing the heat exchangers, structural vibrations, automobile, offshore structures and so on. The investigation of the complex flow structures of the finite circular cylinder can be found a lot. The Kármán vortex shedding from both sides of the cylinder, the horseshoe vortex and base vortex near the ground plane [3], [7] and a pair of streamwise counter-rotating tip vortices generating from the free end [8]-[10] can be observed. Lee [11] also informed that the structures of Kármán vortex cell are reduced related to the aspect ratio when the aspect ratio decreases. The tip-vortices [12]-[14] and a horseshoe vortex [15], [16] exist around a low-aspect-ratio cylinder, while alternating vortex shedding, i.e., Kárman street, cannot be found. In the case of a lower aspect ratio, “arch-type vortex” structure appears behind the cylinder [11] since the vortex from the free-end surface is influenced by the vortices shedding from the sides before reattaching to the ground. Sumner [17] and Porteous et al. [18] report details about the wake structures of finite-height cylinder. Recently, Rinoshika et al. [19]-[21] used the two-dimensional PIV measurement to clarify the wake structures, and proposed inclined holes and a horizontal hole to control the flow around the low-aspect-ratio cylinder. Until now, most of the researches on the 3D wake structures behind a finite-height cylinder are performed based on the two-dimensional PIV measurement. Based on the two-dimensional PIV measurement, Pattenden et al. [4] analysed the mean flow fields behind a finite cylinder of an aspect ratio 1 and gave an arch vortex structure. Beside of horseshoe vortex and tip vortices, a large-scale stump arch vortex behind the cylinder is observed. Recently, Zhu et al. [22] firstly applied Tomographic PIV of six cameras (2058 x 2456 pixels^2) to measure the 3D flow structures around a short wall-mounted cylinder (diameter=20mm) having an aspect ratio of 2. They first found that the arch vortex exhibits 3D M-shape behind the cylinder. It indicates that the shape of arch vortex may depend on the aspect ratio of the short cylinder, which is a very interesting and

challenging problem and thus becomes a target of this study.
In order to clarify the 3D wake flow structures of low-aspect-ratio cylinders, the three-dimensional velocity fields, originated a short circular cylinder of a diameter D = 70 mm (aspect ratio of 1), are firstly measured by Tomographic PIV of high-resolution cameras in a water tunnel. The measured 3D velocity distribution, the vorticity, the Q criterion, the rear separation region and the characteristic of arch type vortex and tip vortices are analysed.

2 Experimental apparatus and Tomographic PIV Setup

Our experiment was performed in a circular open water tunnel. The test section has a size of 3000 mm (length) x 600 mm (width) x 700 m (height). As shown in Fig.1, a short circular cylinder with a height of H =70mm and a diameter of D = 70 mm (the aspect ratio of H/D = 1) was placed on the central axis of the bottom wall 1200 mm downstream of the test section entrance. The streamwise, spanwise and longitudinal directions were respectively indicated by the x, y, and z axes. The centre of the cylinder bottom surface is defined as the origin of the coordinate system. A free stream velocity was fixed at U = 0.162 m/s, corresponding to Reynolds number Re ($\equiv UD/\nu$) of 8,570. The experimental apparatus for the tomographic PIV measurements are shown in Fig.2. The PIV tracer particles of a mean diameter 10 μm were adopted. Illumination was provided by a dual-head Nd:YAG laser (500 mJ/pulse, 532 nm wavelength) with a pulse separation time of 3 ms, which yields average displacements of approximately 0.48 mm (8 pixels) in the free-stream region. The optical lenses and the mirror were designed to generate an 80 mm thick light sheet illuminating the tracer particles around the cylinder. The light sheet was perpendicular to the test section bottom. Four high-resolution (6600 x 4400 pixels^2, 12bit) double-exposure CCD cameras (IMPERX SM-CCDB29M2) were applied to record the measurement domain simultaneously, and the viewing angles were approximately 47^0 between cameras. The laser and cameras were controlled by a synchronizer and the sampling frequency was set at 0.25 Hz.
The measurement volume was in the coordinate range [-115; 130], [-70; 70], [0; 100] (mm) with a digital imaging resolution of 0.075 mm per pixel, so that its corresponding physical domain had a size of 245 x 140 x 100 mm^3. Tomographic PIV was applied in the present investigation for its ability to display the distribution of average and instantaneous three-dimensional velocity. The 3D vector calculation was performed through a multi-pass correlation analysis with a deforming interrogation window. In the final pass, the interrogation volume was 32 x 32 x 32 voxel with 50% overlap, resulting in to a spatial resolution of 2.4 mm and a vector pitch of 2.4 mm.

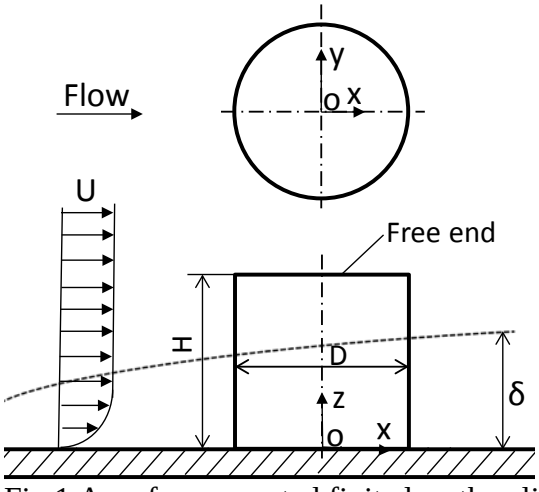

Fig.1 A surface mounted finite length cylinder model

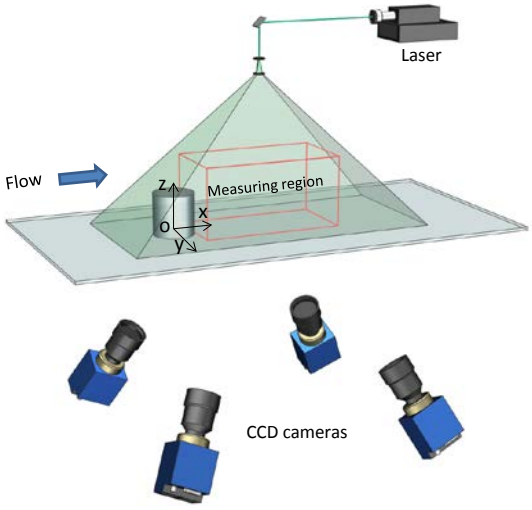

Fig.2 Tomographic PIV setup

3 Results and discussion

Figure 3 shows the 3D isosurface of *u/U*=0 and the time-mean contour of the streamwise velocity behind the short cylinder. The isosurface of *u/U*=0, which is averaged over 300 snapshots, exhibits the 3D rear recirculation zone. Near the plane of *y/D*=0, a lower surface is clearly identified, which corresponds to Zhu et al. [22]. Such concavity region is formed due to the downwash flow from the free end surface. The recirculation zone gradually contracts along the main flow direction, and comes to an end at the downstream location of about *x/D*= 1.6 owing to the interaction of the vortex shedding from the cylinder sidewall and free end.

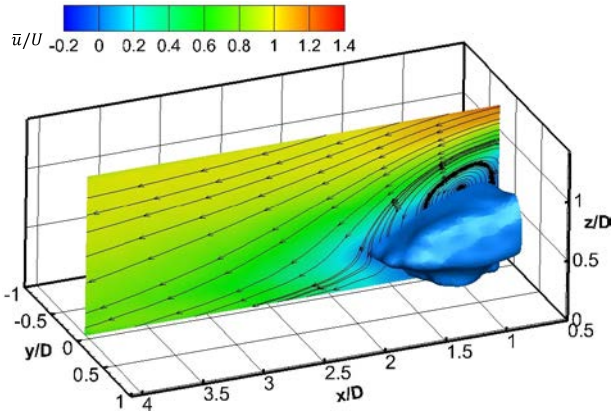

Fig.3 The mean isosurface of $\bar{u}/U$=0 with the streamlines and contour of the streamwise velocity

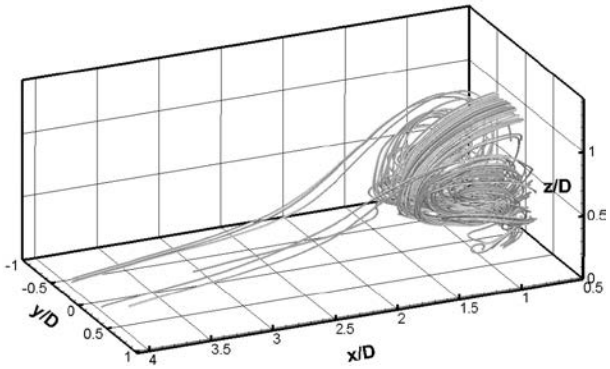

Fig.4 The 3D mean streamlines

Figure 4 shows the 3D mean streamlines of rear recirculation zone near the short cylinder. A 3D large-scale vortex is evidently exhibited, and the centre line of the large-scale vortex is bent in the form of half circle. The vortex diameter at the centre plane of *y/D*=0 is the largest and shrinks close to the ground plane due to the interaction between the vortex shedding from the cylinder sidewall and ground plane.

It is a well-known that the tip vortex pair originating from the free end is a kind of important vortices in the wake of the finite-length cylinder. Figure 5 displays the 3D isosurface of mean streamwise *x*-vorticity of $\bar{\omega}_x D/U = \pm 0.7$ behind the short cylinder, which is plotted as red and blue indicating positive and negative vortex, respectively. A streamwise vortex pair occurring from the free end surface is evidently extracted from TPIV. The streamwise vortex pair exhibits a dipole type and extends downstream to the ground plane due to the effect of the downwash flow.

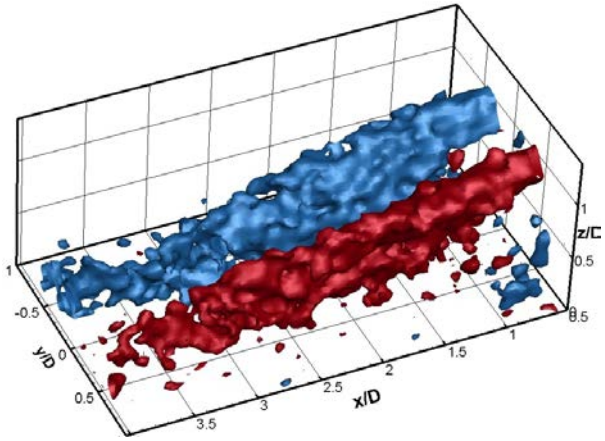

Fig.5 The isosurface of streamwise vorticity $\bar{\omega}_x D/U = \pm 0.7$

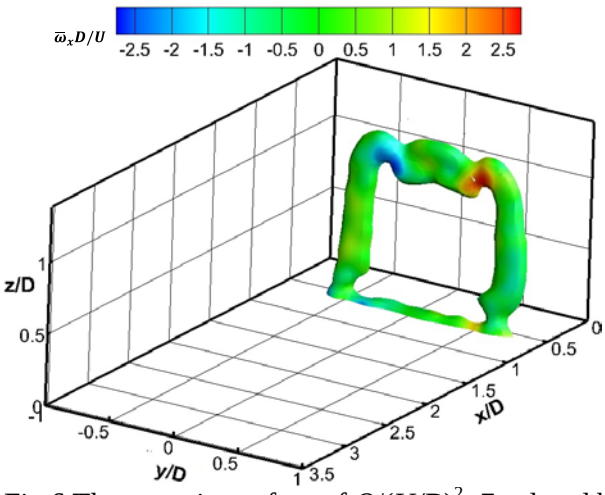

Fig.6 The mean isosurface of $Q/(U/D)^2$=7 colored by the streamwise vorticity $\bar{\omega}_x D/U$

It is a well-known fact that the arch vortex exists in the low-aspect-ratio cylinder wake [4]. Zhu et al. [22] had experimentally confirmed the existence of the 3D arch vortex in the cylinder wake with an aspect ratio of 2 by TPIV. In this study, we also use the *Q* criterion to extract the arch vortex structure and its main features in the cylinder wake with an aspect ratio of 1.
The *Q* criterion is calculated by

$$Q = (\|\Omega\|^2 - \|S\|^2)/2 \quad (1)$$

Where Ω and *S* represent the tensor of the angular velocity and the tensor of strain rate, respectively. $\| \ \|$ shows the Euclidean norm. The *Q* criterion may be used to identify the vortical structures by the excess rotation relative to the strain rate, which is normalized by $(U/D)^2$ in this study.
Figure 6 shows the 3D isosurface distribution of $Q/(U/D)^2$=7 colored by the streamwise vorticity $\bar{\omega}_x D/U$ in the time-averaged flow field. The arch vortex structure clearly exhibits a W-type head instead of a reversed U [4] or an M shape [22] standing on the ground plane behind the short cylinder. Two concave parts near the two sides of the horizontal part are evidently observed in W-type arch structure, which is caused by the downward flow from the free end and tip vortex. The center convex of the horizontal part on the W-type arch structure is induced owning to the strong upwash effect of the large flow separation behind the cylinder as indicated in Fig.6. Being different from M-sharp [22], the larger distance between two tip vortices results in the weaker effect of tip vortices on center part of the head even though they have strong vorticity at the two sides of the arch head, which is described later.

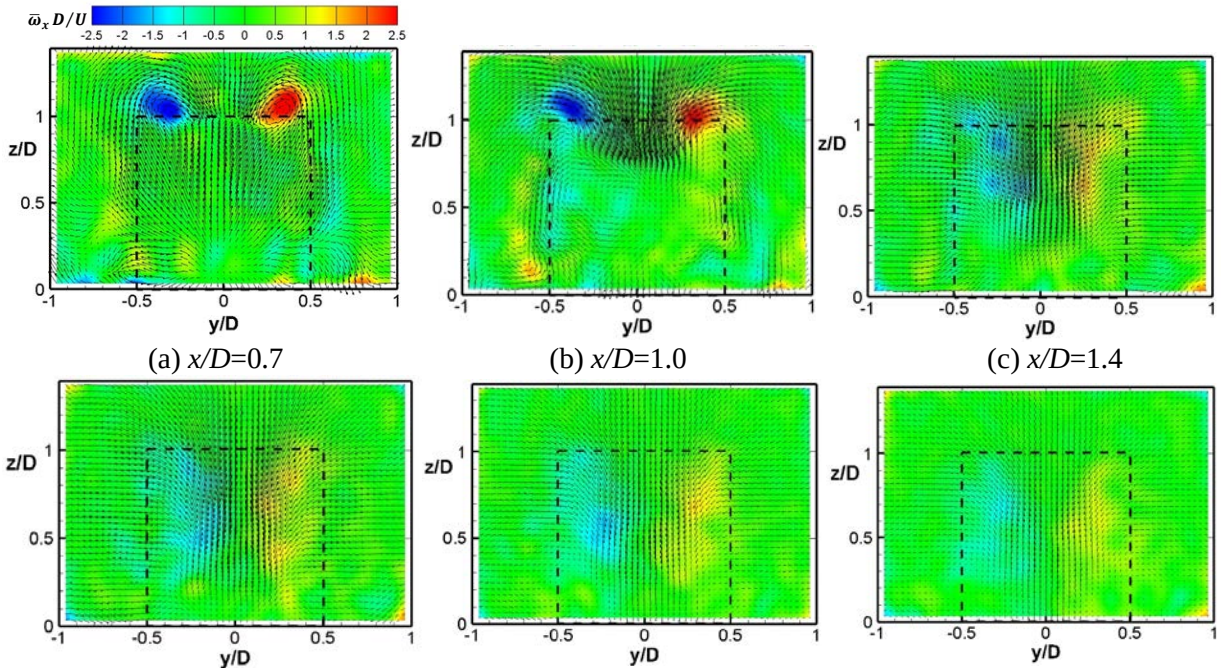

(a) *x/D*=0.7 (b) *x/D*=1.0 (c) *x/D*=1.4

(d) *x/D*=1.8 (e) *x/D*=2.2 (f) *x/D*=2.7

Fig.7 The mean velocity vectors with the contour of the mean streamwise vorticity $\bar{\omega}_x D/U$ in the (*y*, *z*)-plane

The time-averaged velocity vectors with the contour of the streamwise vorticity $\bar{\omega}_x D/U$ in the (*y*, *z*)-plane at *x/D*=0.7, 1.0, 1.4, 1.8, 2.2 and 2.7 are plotted in Fig.7, which visualizes the distribution of 3D velocity and vorticity fields (Fig.4) in the rear view planes. At the location of *x/D*=0.7, a pair of tip vortices can be clearly observed. The upwash and downwash flows can be seen between two tip vortices near the top surface the cylinder, which is an important reason forming the W-type head of arch structure. As going downstream at *x/D*=1.0, the strong downwash is found near the free end surface and two tip vortices are deformed. It is inferred that the W-type head of arch vortex is destroyed at this location. At the downstream locations of *x/D*=1.4 and 1.8, two tip vortices become dispersed and go down due to the effects of the downwash flow and other vortices. Meanwhile their vorticity intensity decreases evidently and becomes weak. At the further downstream of *x/D*=2.2 and 2.7, two tip vortices further decrease and approach to the ground plane.

4 Conclusions

To clarify the 3D flow structures behind a wall-mounted short cylinder, the Tomographic PIV measurements are carried out in this study. The main results are shown as follows.

(1) A 3D W-type arch vortex is first found behind short cylinder. The “head” of the horizontal part is induced by the upwash flow of the large flow separation, and the “shoulders” of the horizontal part are caused by the downward flow and tip vortices.

(2) The horizontal shape of arch vortex structure does not only depend on the aspect ratio of cylinder, but also is related to the cylinder diameter.

5 Acknowledgment

The first author (HR) gratefully acknowledges support from JSPS Research Fellowships for Young Scientists (2019~2022). The second author (AR) wishes to acknowledge the support given to him by Grant-in-Aid for Scientific Research (C) (no.16K06067) from the Japanese Society for the Promotion of Science and Natural Science Foundation of China (Grant No. 11721202 and 11772035).
The authors also wish to acknowledge Dr. C.Y. Wang, Mr. H.Y. Zhu and Mr. X.L. Han, Beijing University of Aeronautics and Astronautics, for their helps in the Tomographic PIV experiments.

References

[1] A. Rinoshika, Y. Zhou, Orthogonal wavelet multi-resolution analysis of a turbulent cylinder wake, Journal of Fluid Mechanics, 524 (2005) 229-248.

[2] A. Rinoshika, Y. Zhou, Reynolds number effects on wavelet components of self-preserving turbulent structures, Physical Review E 79 (2009) 046322 1–11.

[3] D. Sumner, J.L. Heseltine, O.J.P. Dansereau, Wake structure of a finite circular cylinder of small aspect ratio, Experiments in Fluids, 37 (2004) 720–730.

[4] R.J. Pattenden, S.R. Turnock, X. Zhang, Measurements of the flow over a low-aspect-ratio cylinder mounted on a ground plane, Experiments in Fluids, 39 (2005) 10-21.

[5] H.F. Wang, Y. Zhou, The finite-length square cylinder near wake, Journal of Fluid Mechanics, 638 (2009) 453–490.

[6] R.T. Gonçalves, G.R. Franzini, G.F. Rosetti, J.R. Meneghini, A.L.C. Fujarra, Flow around circular cylinders with very low aspect ratio, Journal of Fluids and Structures, 54 (2015) 122–141.

[7] S. Tanaka, S. Murata, An investigation of the wake structure and aerodynamic characteristics of a finite circular cylinder, JSME International Journal, Series B: Fluids Thermal Engineering, 42 (1999) 178–187.

[8] T. Kawamura, M. Hiwada, T. Hibino, T. Mabuchi, M. Kumada, Flow around a finite circular cylinder on a flat plate, Bulletin of the JSME, 27 (1984) 2142–2150.

[9] C.R. Johnston, D.J. Wilson, A vortex pair model for plume downwash into stack wakes, Atmospheric Environment, 31 (1996) 13–20.

[10] M.S. Adaramola, O.J. Akinlade, D. Sumner, D.J. Bergstrom, A.J. Schenstead, Turbulent wake of a finite circular cylinder of small aspect ratio, Journal of Fluids and Structures, 22 (2006) 919–928.

[11] L.W. Lee, Wake structure behind a circular cylinder with a free end, In: Proceedings of the Heat Transfer and Fluid Mechanics Institute, (1997) 241–251.

[12] T. Okamoto, M. Yagita, The experimental investigation on the flow past a circular cylinder of finite length placed normal to the plane surface in a uniform stream, Bulletin of the JSME, 16 (1973) 805–814.

[13] T. Kawamura, M. Hiwada, T. Hibino, T. Mabuchi, M. Kumada, Flow around a finite circular on flat

plate: in the case of cylinder length larger than turbulent boundary layer thickness, Transactions of the JSME, 50 (1984) 332–341. (in Japanese).

[14] S.C. Roh, S.O. Park, Vortical flow over the free end surface of a finite circular cylinder mounted on a flat plate, Experiments in Fluids, 34 (2003) 63–67.

[15] S. Krajnović, Flow around a tall finite cylinder explored by large eddy simulation, Journal of Fluid Mechanics, 676 (2011) 294–317.

[16] N. Rostamy, D. Sumner, D.J. Bergstrom, J.D. Bugg, Local flow field of a surface-mounted finite circular cylinder, Journal of Fluids and Structures, 34 (2012) 105-122.

[17] D. Sumner, Flow above the free end of a surface-mounted finite-height circular cylinder, A review, Journal of Fluids and Structures, 43 (2013) 41-63.

[18] R. Porteous, D.J. Moreau, C.J. Doolan, A review of flow-induced noise from finite wall-mounted cylinders, Journal of Fluids and Structures, 51 (2014) 240–254.

[19] H. Rinoshika, A. Rinoshika, S. Fujimoto, "Passive control on flow structure around a wall-mounted low aspect ratio circular cylinder by using an inclined hole", Bulletin of the JSME, Journal of Fluid Science and Technology, 12 (2017) 1-13.

[20] H. Rinoshika, A. Rinoshika, Effect of a horizontal hole on flow structures around a wall-mounted low-aspect-ratio cylinder, International Journal of Heat and Fluid Flow, 71 (2018) 80–94.

[21] H. Rinoshika, A. Rinoshika, S. Fujimoto, Visualization of a finite wall-mounted cylinder wake controlled by a horizontal or inclined hole, Journal of Visualization, 21 (2018) 543-556.

[22] H. Y. Zhu, C. Y. Wang, H. P. Wang and J. J. Wang, Tomographic PIV investigation on 3D wake structures for flow over a wall-mounted short cylinder, Journal of Fluid Mechanics, 831 (2017) 743-778.